

Decoherence and Full Counting Statistics in a Mach-Zehnder Interferometer

Heidi Forster¹, Sebastian Pilgram^{1,2}, and Markus Buttiker¹

¹Departement de Physique Théorique, Université de Genève, CH-1211 Genève, Switzerland

²Theoretische Physik, ETH Zurich, CH-8093 Zurich, Switzerland

(Dated: March 23, 2024)

We investigate the Full Counting Statistics of an electrical Mach-Zehnder interferometer penetrated by an Aharonov-Bohm flux, and in the presence of a classical fluctuating potential. Of interest is the suppression of the Aharonov-Bohm oscillations in the distribution function of the transmitted charge. For a Gaussian fluctuating field we calculate the first three cumulants. The fluctuating potential causes a modulation of the conductance leading in the third cumulant to a term cubic in voltage and to a contribution correlating modulation of current and noise. In the high voltage regime we present an approximation of the generating function.

I. INTRODUCTION

For two decades theoretical and experimental investigations of the noise properties of small electrical conductors have been an important frontier of mesoscopic physics¹. Non-equilibrium noise, in particular shot noise^{2,3,4,5} can provide information on physical properties which are not accessible from conductance measurements. Recently there has been considerable interest in characterizing transport in mesoscopic systems not only via conductance and noise but also with all higher order current correlations. This is achieved by deriving a generating functional from which the quantities of interest can be obtained simply by taking derivatives. To construct the generating functional, it is useful to imagine that electrons passing the sample in a given time are counted, and the approach is thus known as Full Counting Statistics^{6,7}. While initial work was based on the scattering approach to electrical transport, subsequently a number of different methods have been developed. These include an approach based on Keldysh Green's functions^{8,9,10,11}, the non-linear sigma model¹², an approach based on a cascade of Boltzmann-Langevin equations¹³ and a formulation in terms of a stochastic path integral^{14,15,16,17,18,19,20,21,22}. These later methods are principally useful if the quasi-classical part of the transport coefficients is dominant. A first experiment²³ has given additional impetus for this research. It has stimulated work which treats the effect of the measurement circuit on the counting statistics²⁴ and led to proposals for novel detection schemes^{25,26,27}.

In this work we are interested in the Full Counting Statistics (FCS) of transport problems in which quantum effects are important. For instance, in single channel mesoscopic conductors quantum interference is essential. In such a situation, transport becomes classical only due to dephasing. It is thus interesting to examine the effect of inelastic processes on the counting statistics of a single channel problem and to investigate the transition from quantum mechanical transport to fully classical transport.

The central aim of our work is thus the derivation of the generating functional in the presence of inelastic scat-

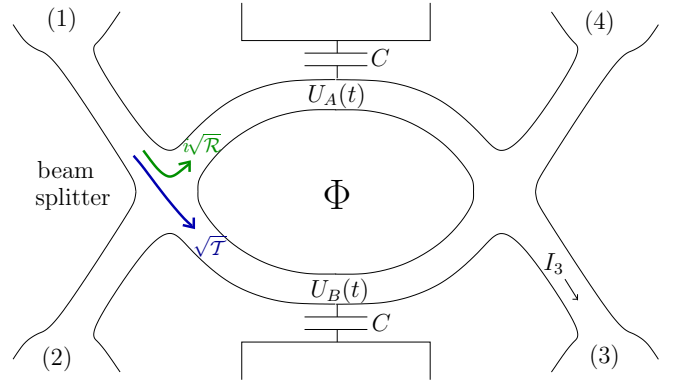


FIG. 1: The Mach-Zehnder interferometer: a four-terminal AB-ring, threaded by a magnetic flux. The interferometer arms are coupled to classical fluctuating potentials modeling the effect of dephasing. The influence of dephasing on current fluctuations in lead 3 is investigated.

tering. We investigate an interferometer penetrated by an Aharonov-Bohm flux and subject to a random classical fluctuating potential. For simplicity we assume that the interferometer is of the Mach-Zehnder (MZI) type (Fig. 1), an interferometer without backscattering. In such a system there are no closed orbits and thus only a finite number of possible trajectories.

Despite these simplifying assumptions the derivation of the generating functional is a non-trivial problem. To investigate the effect of the fluctuating potential, a time-dependent treatment of transport is needed together with a technique of statistical averaging. In fact, in the present work we are able to give the generating functional only in the limiting case of the high voltage regime. In the general case, we present results for the first three cumulants.

The model we investigate is closely related to earlier work by Seelig et al. on the effect of dephasing on the conductance²⁸ and four-terminal resistances in ballistic interferometers²⁹. In few channel structures dephasing might be sample specific²⁹. Experimental investigations on dephasing in ballistic interferometers is provided by Hansen et al.³⁰ and Kobayashi et al.³¹. Recently an elec-

tronic MZI has been experimentally realized by Jiet al.³², using edge states in the quantum hall regime. This experiment also raised interesting questions on the shot noise of the interferometer and dephasing. The effect of dephasing on shot noise in such an interferometer has been discussed by Marquardt and Buder based on classical³³ and quantum³⁴ fluctuating field models.

Still another motivation for the work presented here derives from recent proposals to implement orbital entanglement³⁵ based on electron-hole generation³⁶ in two-particle intensity-interferometers³⁷. In these proposals quantum interference effects play an important role in noise and higher order correlations³⁸.

II. THE MACH-ZEHNDER INTERFEROMETER

The conceptually simplest system displaying electron interference is the electronic Mach-Zehnder interferometer. The setup is shown in Fig. 1, it consists of two beam splitters connected by two interferometer arms enclosing a magnetic flux. Each beam splitter is characterized by a transmission amplitude T for an electron going straight through, and a reflection amplitude iR , with $R + T = 1$. The simplicity of the interferometer originates from the exclusion of backscattering which discards closed orbits and separates completely the processes of left and right moving particles.

Interference occurs, because the different vector potentials in the two arms lead to a phase difference between the paths A and B. This difference creates a characteristic flux-periodicity in the interference pattern, the Aharonov-Bohm effect.

In our work, dephasing is introduced with the help of classical fluctuating potentials, $U_A(t)$ and $U_B(t)$. The correlation function of these fluctuating potentials can be self-consistently determined treating electron-electron interactions in a random phase approximation²⁸. Here we take this correlation function to be given. The potentials cause the particles to pick up an additional time-dependent phase $\phi_i(t) = \int_{t_0}^t dt U_i(t)$, $i = A$ or B (here and in the following we set $e = \hbar = 1$). We assume, that the traversal time of the particles is not affected by the potentials. The transmission amplitudes of particles entering the interferometer at time t in lead α and leaving it at time t^0 in lead β are collected in the time-dependent scattering matrix³⁹ $S_{\beta\alpha}(t; t^0)$. For a one-channel MZI this scattering matrix is four dimensional and has special properties: as backscattering is excluded, the scattering matrix has non-vanishing elements only in the off-diagonal 2×2 blocks. Because the motion is purely ballistic, the scattering matrix depends effectively on one

single time $S_{\beta\alpha}(t; t^0) = \langle \hat{c}_{\beta}^\dagger(t) \hat{c}_{\alpha}(t^0) \rangle S(t)$, where

$$\begin{aligned} S_{31}(t) &= iRT \overline{(e^{i\phi_A(t)} + e^{i\phi_B(t)} + 1)} \\ S_{32}(t) &= T e^{i\phi_A(t)} R \\ S_{41}(t) &= R e^{i\phi_B(t)} T \\ S_{42}(t) &= iRT \overline{(e^{i\phi_A(t)} + e^{i\phi_B(t)} + 1)} \end{aligned} \quad (1)$$

Here we assumed equal arm lengths and introduced the phase difference $\phi(t) = \phi_A(t) - \phi_B(t)$ and the magnetic flux in units of the flux quantum. The remaining four elements are found from the magnetic field symmetry of the scattering matrix $S(-) = S^*(+)$.

Without the fluctuating potentials the system is coherent: $\phi(t) = 0$. The transmission probability becomes $T_{31} = \mathcal{P}_{31} = 2RT(1 + \cos \phi)$ and shows cosine oscillations in flux. Such AB-oscillations are visible in conductance experiments.

When we include dephasing by the fluctuating potentials, the scattering matrix becomes time-dependent and the quantities of interest have to be averaged over the statistically distributed potential. This average suppresses the AB-oscillations. For the case of conductance and noise, these effects have been studied in detail^{28,33}. In this work we will generalize this discussion to higher order current correlations (Full Counting Statistics).

III. FCS OF THE COHERENT SYSTEM

The Full Counting Statistics⁷ (FCS) is the distribution function $P(Q)$ giving the probability that a certain charge $Q = \int_{t_0}^{t_0+t} dt I(t)$ flows through a system during the observation time t_0 . Its Fourier transform is called its generating function $\chi(\lambda)$, the conjugated variable λ is named the counting field:

$$\chi(\lambda) = \sum_Q P(Q) e^{i\lambda Q} \quad (2)$$

$$P(Q) = \frac{1}{2\pi} \int_{-\pi}^{\pi} d\lambda \chi(\lambda) e^{-i\lambda Q} \quad (3)$$

The expansion of $\ln \chi(\lambda)$ in λ yields all irreducible cumulants: $\ln \chi(\lambda) = \sum_k \frac{(i\lambda)^k}{k!} C^k$. For large t_0 the first cumulant gives the mean current $\langle I \rangle = \langle I \rangle_{t=t_0}$, the second cumulant is the zero frequency noise $C^2 = \langle Q^2 \rangle_{t=t_0}$, the third cumulant $C^3 = \langle Q^3 \rangle_{t=t_0}$ describes the asymmetry (skewness) of the distribution, and so on. The generating function provides in principle a complete description of the zero-frequency current fluctuations.

We consider a four-terminal conductor, thus Q and λ are four dimensional vectors. Since in the MZI current conservation relates current fluctuation of all leads, it is in most cases sufficient to concentrate on the charge distribution in one lead. In the following we will choose lead 3 and call Q its charge and λ the corresponding counting variable.

In the coherent regime ($\Gamma(t) = 0$), the scattering matrix is time independent, and the calculation of the generating function is straightforward. Following the work of Levitov and Lesovik⁷, one defines an energy-dependent 4×4 matrix $A = f^{-1} S^{-1}$, where the diagonal matrix $f = f(E)$ contains the Fermi functions of the four terminals. S incorporates the counting fields by phase shifts $S = e^{i(\frac{Q}{2} - \Phi)} S$ (remember that $\Phi = \frac{2\pi}{\phi}$). The generating function is

$$\ln \langle \rangle = \frac{t_0}{2} \int dE \text{tr} \ln(1 + A) : \quad (4)$$

Because backscattering is excluded, the matrix A is block diagonal, and \ln separates into two independent contributions. This fact expresses the statistical independence of left and right going particles.

For a two-terminal conductor, the FCS can always be interpreted as a classical binomial distribution. For a four terminal conductor like the MZI this is in general no longer the case. There exists however a special configuration: at zero temperature a voltage V is applied on terminal 1 and zero voltage on the other terminals. In this case only two processes exist: transmission from terminal 1 into lead 3 with probability T_{31} or into lead 4 with probability $1 - T_{31}$. The number of incident particles during the time t_0 is given by $N = \frac{V t_0}{2}$. We then recover the binomial distribution of the two-terminal conductor

$$\langle \rangle = (e^{i\Phi} T_{31} + (1 - T_{31}))^N \quad (5)$$

$$P(Q) = \sum_Q \binom{N}{Q} T_{31}^Q (1 - T_{31})^{N-Q} \quad (6)$$

with the only difference, that the transmission probability $T_{31} = 2R_T(1 + \cos \Phi)$ depends on the magnetic flux. Consequently the distribution function $P(Q)$ contains all harmonics up to $\cos N\Phi$. The flux periodicity of $P(Q)$ is shown in Fig. 2 (a). For symmetric beam splitters and certain values of Φ , all particles end up in one lead, due to complete constructive interference. The distribution is then singular and noiseless: $P(Q) = \delta_{Q,N}$ for $\Phi = 2k\pi$, and $P(Q) = \delta_{Q,0}$ for $\Phi = (2k+1)\pi$ with $k \in \mathbb{Z}$.

At finite temperature this simple binomial picture is modified and does not coincide with the two-terminal conductor statistics⁶. We obtain

$$\langle \rangle = \exp \left[\frac{t_0 k_B T}{2} \text{arccosh}^2 u(\Phi) - \frac{v^2}{2} + i v \frac{3}{4} \Phi \right] \quad (7)$$

with $v = \frac{V}{2k_B T}$ and the complex function $u(\Phi) = T_{31} \cosh v + i \frac{1}{2} + (1 - T_{31}) \cosh v - i \frac{1}{2}$.

Fig. 2 (b) shows plots of the logarithm of the distribution function for finite temperature. At high temperatures the flux dependence is strongly reduced, as is to be expected for a general interferometer. But the MZI with arms of equal lengths investigated here has the special property that it is described by energy-independent transmission probabilities. Thus the con-

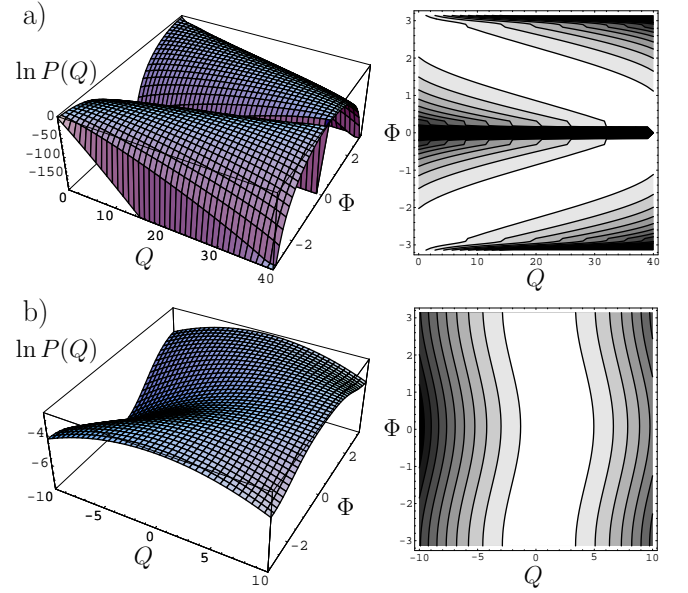


FIG. 2: (a) The distribution function at zero temperature (logarithmic scale, $V t_0 = 2\pi = 40$). Left: 3D plot of the binomial distribution, which is periodic in flux. Right: the same in contour representation, dark areas correspond to low probability. (b) The distribution function at high temperature $k_B T = 10V$ (for a long observation time $t_0 k_B T = 100$). The flux dependence is washed out, and the distribution tends towards a Gaussian.

ductance does not suffer from energy averaging and exhibits full Aharonov-Bohm oscillations even at high temperatures. However, the distribution function becomes classical, because the high-temperature fluctuations of transmitted charge are dominated by two-particle processes, whose probability is flux independent and equal to one.

At very high temperatures $k_B T \gg V$, we find a Gaussian function $P(Q) \approx e^{-\frac{(Q - \langle Q \rangle)^2}{2\sigma^2}}$ with $\sigma^2 = \frac{t_0 k_B T}{2}$, centered around the mean charge $\langle Q \rangle = \frac{t_0}{2} T_{31} V$.

IV. INFLUENCE OF DEPHASING

We now start to consider the influence of the fluctuating potential on the FCS. The scattering matrix becomes time-dependent, and the electrons can be scattered between different energies. Following the idea of Ivanov and Levitov⁴⁰, the different energies can be viewed as an infinite number of independent scattering channels. Switching to time-representation $S(t; t^0) = (e^{i\Phi(t-t^0)} S(t))$, this leads to a generalization of formula (4) for the generating function, where we extend the usual trace (tr) to a trace in time-space (Tr) including time integration:

$$\ln \langle \rangle = \text{Tr} \ln(1 + A) \quad (8)$$

All matrices are defined in analogy to section III: The matrix A depends on two time-variables $A(t^0; t) = n(t^0 - t)(S^V(t)S(t) - 1)$; the diagonal matrix n contains the Fourier transforms of the Fermi functions in the four terminals $n = n(t - t^0) = \frac{dE}{2} f(E) e^{iE(t - t^0)}$. It can easily be checked, that Eq. (8) reduces to Eq. (4), when A depends only on time-differences (elastic scattering).

To study the influence of dephasing on the generating function, it has to be averaged statistically over all possible realizations of the fluctuating potential: $\langle \dots \rangle_U = \int dU e^{\text{Tr} \ln(1 + A)} \dots$. For a Gaussian distribution, this average is expressed by a functional integral

$$\langle \dots \rangle_U = \int \mathcal{D}U \int \mathcal{D}\bar{U} \int \mathcal{D}\psi \int \mathcal{D}\bar{\psi} e^{-\frac{1}{2} \int_0^{R\tau_0} dt \int_0^{R\tau_0} dt' U(t) K(t - t') U(t')} \dots \quad (9)$$

The kernel K is defined via $K(t) = \frac{d!}{2} \int_U^1 (!) e^{i!t}$, with the spectral function of the potential $U(!) = \int dt hU(t) U(0) i e^{i!t}$. Only potential differences matter: $U(t) = U_A(t) - U_B(t)$.

In general the averaging can not be performed analytically. Therefore, in a first step, we expand $\langle \dots \rangle$ in the counting field and calculate the average of single cumulants, crosschecking known results^{28,33} and presenting new results for the third cumulant. In a second step, we will derive directly an expression for $\langle \dots \rangle$ in the case of a slowly fluctuating potential.

V. CUMULANTS, EXACT AND LIMITING CASES

The effect of the averaging on the cumulants is determined by three quantities: the correlation time τ_{RC} of the fluctuating potential $U(t)$, the traversal time τ , and a decoherence parameter z .

τ_{RC} is typically the RC-time, with C the coupling capacitance, and R the charge relaxation resistance⁴¹; it provides a cut-off frequency for energy exchanges between particles and fluctuating potential. The traversal time τ is the correlation time of the phase $\phi(t)$, because the electrons integrate the fluctuating potential $U(t)$ during time τ . For τ_{RC} the correlation function of the phase is a triangle in time⁴² $\langle \phi'(t) \phi'(0) \rangle = \frac{U}{2} \left(1 - \frac{|t|}{\tau_{RC}} \right)$ with U the spectral function of the potential at zero frequency. This spectral function is given by $U = U^2 \tau_{RC}$, where U is the mean fluctuation amplitude of the potential. Because the relevant quantity in the MZI is the accumulated phase $\phi(t)$, it is convenient to introduce the reduced mean fluctuation amplitude $U = \frac{U}{\tau_{RC}}$. The spectral function U depends for a Gaussian fluctuating field $U(t)$ on the decoherence parameter z via^{28,33,43}:

$$z = \exp\left(-\frac{U}{2}\right) \quad (10)$$

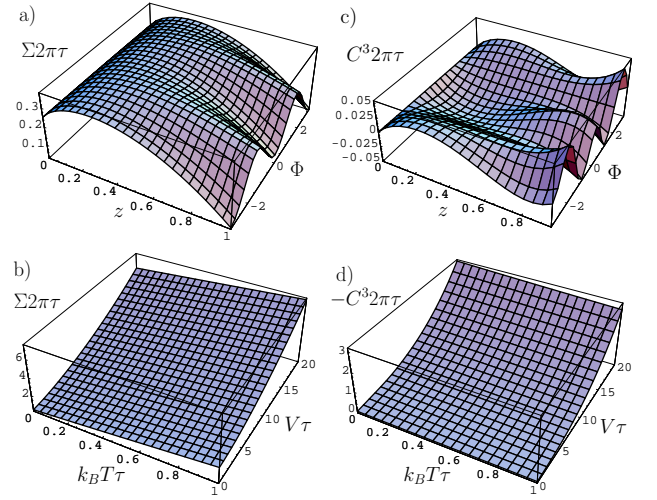


FIG. 3: Noise (a), ($k_B T = 0$) and third cumulant (c), ($k_B T = 0.1$) as a function of decoherence parameter z and voltage (for $V = 1$): the AB-oscillations are suppressed for decreasing z . (b) and (d) display the dependence on voltage and temperature ($z = 0.3$). The third cumulant changes little with temperature, but the noise shows linear thermal noise for high temperature.

The parameter z indicates the dephasing strength; it varies between 0 for complete dephasing and 1 in the absence of dephasing.

We consider the configuration with V applied on terminal 1, and current fluctuations observed in lead 3. The cumulant of k -th order is given by

$$Q^k = \frac{1}{i^k} \frac{d^k \ln \langle \dots \rangle_U}{d^k} \Big|_{=0} \quad (11)$$

The calculation for the first cumulants is sketched in the appendix A, here we will give only the main results and discuss the figures.

The mean current in lead 3 is linear in voltage, and proportional to the transmission probability, averaged over the potential: $\langle I_3 \rangle = \frac{1}{2} 2R T (1 + z \cos V)$. In comparison to the coherent system, the AB-oscillations in the conductance are suppressed by the decoherence parameter z , in agreement with the work of Seelig and Buttiker²⁸.

The noise has been studied in detail by Marquardt and Bruder³³. The expression for the noise is separated into a Nyquist part Σ_{nyq} , a modulation part Σ_I and a two-particle exchange contribution Σ_{ex} . The V -independent Nyquist noise Σ_{nyq} describes thermal noise⁴⁴ as well as energy exchange between particles and the classical potential $U(t)$ up to the cut-off frequency $1/\tau_{RC}$. It is finite even for zero temperature and voltage. Σ_I is a consequence of the variation of the conductance in time, it grows with V^2 and is temperature-independent. The exchange term Σ_{ex} describes shot noise and is a function of voltage and temperature, vanishing for $V = 0$ and linear for high voltage. Σ_{ex} is a consequence of the indistin-

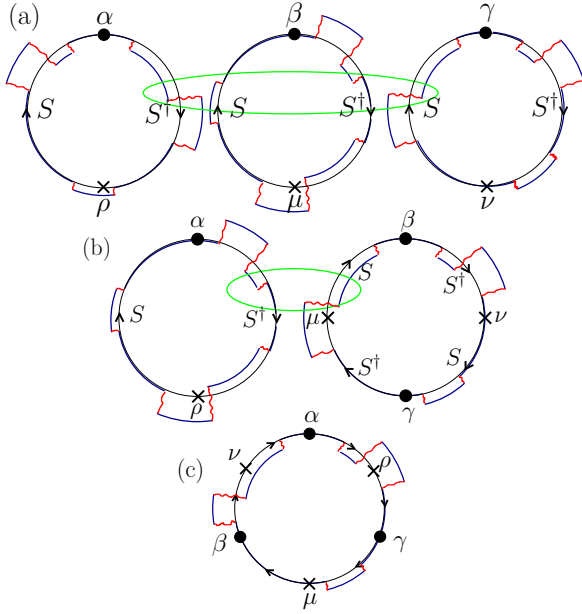


FIG. 4: Processes contributing to the third cumulant at zero temperature. The black points correspond to channels ρ , μ , ν at time $t + \tau$, and the crosses to channels ρ , μ , ν at time t . In C_I^3 (a) three one-particle processes are connected by correlations of the fluctuating potential (circled in grey/green). In (b) the correlation of the modulated current and the shot noise are displayed, which contributes to C_I^3 . C_{3p}^3 (c) is the three particle contribution, averaged over excitations.

guishability of identical particles. Thus the total noise is

$$= n_{\text{nyq}}(T) + C_I^3(V^2) + C_{\text{ex}}^3(V; T); \quad (12)$$

For symmetric beam splitters, the fundamental AB-period is absent in the noise and the AB-oscillations are proportional to $\cos 2\phi$. They are suppressed for $z \neq 0$, compare Fig. 3 (a).

In Fig. 3 (b) the noise is shown as a function of temperature and voltage: it is linear in temperature for high $k_B T$, simply due to thermal noise. The quadratic dependence on voltage does not change with temperature.

In the third cumulant we distinguish three contributions: a modulation part C_I^3 , proportional to V^3 , a second term C_I^3 , that connects current modulation and noise, and a three-particle contribution C_{3p}^3 :

$$C^3 = C_I^3(V^3) + C_I^3(V; T) + C_{3p}^3(V; T) \quad (13)$$

The processes leading to these three contributions can be visualized as shown in Fig. 4. Fig. 4 (a) corresponds to the modulation contribution C_I^3 . Each circle contains the one-particle process creating current in the corresponding lead: In the left half of the first circle an electron, entering the scatterer at time t in lead α is transmitted into lead β at time $t + \tau$ with the amplitude S , it is moving forward in time. Correspondingly in the right half circle a hole is transmitted from lead β into lead α with amplitude S^\dagger ,

moving backward in time. We sum over all channels at the points \times and measure the current at the points \bullet . As we investigate the third cumulant of charge transmitted into lead 3, we have here $\alpha = \beta = \gamma = 3$.

The radial direction can be interpreted as the energy of the particles. Due to the fluctuating potential, we allow energy exchange and average over all excitations during the traversal time under the condition, that the energy takes the value E at point \bullet .

The modulation part C_I^3 consists of three one-particle processes, that are connected via the correlation of the fluctuating potential only.

In the second term C_I^3 a modulated current and the noise are correlated also via the fluctuating potential. In the shot noise (the right ring in Fig. 4 (b)) we have two points \times (time t) and \bullet (time $t + \tau$), because we deal with a two-particle process: an electron propagates from channel α to β , a hole from β to α , an electron from β to γ , and a hole from γ to β . In addition there is {even at zero temperature} a correlation between the modulated current and the Nyquist noise, which is not represented in Fig. 4.

C_{3p}^3 then is the actual three-particle exchange contribution, connecting the leads α , β , and γ by six S-matrices. Here we again average over excitations between the points \bullet .

In Fig. 5 the three contributions and the total third cumulant C^3 are depicted as a function of V . Note that C^3 is negative for $z = 0$ and $z = 0.3$, this implies that the distribution in lead 3 is skewed to the right. For high voltage the term C_{3p}^3 is linear, C_I^3 is quadratic, and the cubic contribution C_I^3 dominates. The full third cumulant is odd in voltage and thus vanishes for $V = 0$.

In the symmetric case, $R = 0.5$, we find AB-oscillations proportional to $\cos 3\phi$ and $\cos \phi$; with decreasing z the terms in $\cos 3\phi$ are stronger damped than those with $\cos \phi$, as shown in Fig. 3 (c). Note also, that around $\phi = 0$; the third cumulant changes sign with decreasing z . Fig. 3 (d) shows the third cumulant as a function of temperature and voltage. In contrast to the noise the third cumulant contains no voltage independent (Nyquist) contribution whatsoever, and therefore, changes little with temperature⁴⁵.

We can distinguish two limiting regimes: high and low voltage³³ in comparison to $1/\tau$. In the first case, many particles ($V \gg 1$) pick up approximately the same phase $\phi'(t)$, since many wave packets enter at the same time into an interferometer arm. To the contrary for low voltage ($V \ll 1$) every wave packet acquires different phases $\phi'(t)$, which are uncorrelated. Therefore, for high and low voltage we can make approximations of a slowly and a fast varying phase $\phi'(t)$ respectively.

We next compare these approximations with the exact expression. The modulation contribution C_I^3 does not depend on the phase dynamics, but is determined by the parameter z . Therefore, it is independent of whether we consider a fast or a slowly varying phase. As C_I^3 decreases with V^3 , in the low voltage regime it is small compared

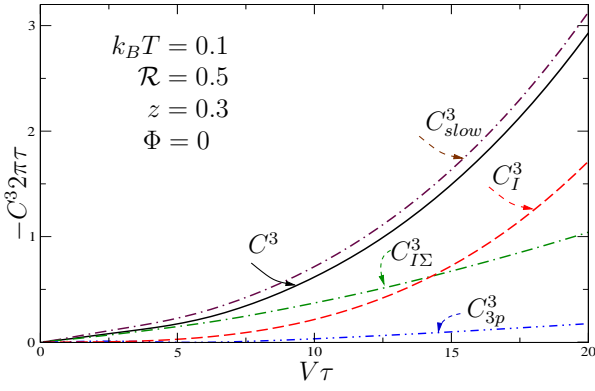


FIG. 5: The third cumulant and its three contributions as a function of voltage. At high V the cubic term dominates. The dashed line C^3_{slow} shows the approximation in the high voltage regime.

to the terms linear in voltage. In both limiting cases the averaging of the contributions C^3_{3p} and C^3_I simplifies; additional details of the averaging and the approximations are discussed in the appendix A.

The low voltage approximation is only for very small values of V , and we will not discuss this limiting case here further. A comparison of the high voltage approximation, detailed in the appendix A, with the exact result is shown in Fig. 5. This approximation matches the exact curve very well for a wide range of V and even in the case $V \rightarrow 1$.

VI. GENERATING FUNCTION IN THE HIGH VOLTAGE REGIME

The discussion above showed that in principle we can calculate any single cumulant with the only assumption of a Gaussian fluctuating potential. However the calculational effort grows very fast with the order of the cumulant. For this reason let us now concentrate on the limiting case of high voltage ($V \rightarrow 1$), when many particles pick up approximately the same phase. In this limit the generating function, Eq. (8) can be evaluated directly. To this end, we perform the averaging, see Eq. (9) under the following two assumptions.

(i) When the accumulated phase $\phi'(t) = \int_t^{t_0} dt' U(t')$ varies slowly, the matrix $A(t; t^0)$ in Eq. (8) takes the form⁴⁶ $A(t; t^0) \approx \exp(i \int_t^{t^0} dt' U(t')) S^y(\phi'(t)) S^x(\phi'(t^0))$. It depends on a time difference and on a parameter ϕ' , that itself is a function of a (single) time variable. After Fourier transformation we are left with one integral in time and another in energy. At zero temperature, the energy integral is easily performed and one obtains

$$\text{Tr} \ln(1 + A) \approx \frac{V}{2} \int_0^{t_0} dt \ln[1 + T_{31}(\phi'(t)) (e^{i\phi'(t)} - 1)] \quad (14)$$

Here $T_{31}(\phi'(t))$ depends on the instantaneous phase $\phi'(t)$.

(ii) To take into account the correlation time of phase fluctuations, we make an additional approximation beyond the slow approximation discussed so far: We take the slowly varying phase $\phi'(t)$ to be a steplike function, that has constant values $\phi' = U$ in time intervals $[k; (k+1)]$ for $k \geq N_0$. The values U and consequently the values T_{31} obey a Gaussian distribution. Note that the parameter U does not describe the actual fluctuations of the potential $U(t)$ since these are determined by the correlation time τ_{RC} which is here assumed to be smaller than τ .

The $t_0 =$ time intervals of length τ that can be treated independently. During each time interval the functional integral (9) becomes a simple Gaussian integral in the variable U :

$$\langle \dots \rangle_U = \int_{-\infty}^{\infty} dU \frac{e^{-\frac{U^2}{2}}}{\sqrt{2\pi}} (1 + T_{31}(U) (e^{i\phi'(t)} - 1))^N A; \quad (15)$$

with $T_{31}(U) = 2RT(1 + \cos(\phi'(t) + U))$. The integration in U leads to the generating function

$$\langle \dots \rangle_U = \sum_{m=0}^{\infty} \frac{(-1)^m}{m!} \left(\frac{N}{2} \right) \left(\frac{N}{2} + \frac{1}{2} \right) \left(\frac{ab}{4c^2} \right)^m \quad (16)$$

with the constants $c = 1 + 2RT(e^{i\phi'(t)} - 1)$, $a = RT e^{i\phi'(t)} (e^{i\phi'(t)} - 1)$, $b = RT e^{-i\phi'(t)} (e^{i\phi'(t)} - 1)$.

This approximation for the generating function applies also in the case $\tau_{RC} > \tau$: then the correlation time of the phase $\phi'(t)$ is the same as the one of the potential $U(t)$, τ_{RC} , and the time τ in Eq. (16) has to be replaced by τ_{RC} .

Starting from this generating function (16) one finds immediately the cumulants by simply taking derivatives in ϕ' . These cumulants in their modulation contributions from the slow limiting case of the cumulants presented in section V, due to the treatment of $\phi'(t)$ as a steplike function (corresponding to a discretization in time space).

Each cumulant shows harmonic oscillations in ϕ' up to the order of the derivative. As expected the terms containing oscillations with higher periodicity are damped stronger. Therefore, Eq. (16) is a convenient starting point to investigate the strong dephasing limit. In this case we can restrict the sum in Eq. (16) to small powers in z . Up to first order in z the generating function consists of two hypergeometric functions F

$$h(\phi')_U = c^N F\left(\frac{N}{2}; \frac{N}{2} + \frac{1}{2}; 1; \frac{ab}{4c^2}\right) + c^N {}_1F_1\left(c-1; c-1; z \cos \phi' F\left(\frac{N}{2} + \frac{1}{2}; \frac{N}{2} + 1; 2; \frac{ab}{4c^2}\right)\right) \quad (17)$$

The first term represents the purely classical part, it does not depend on z and ϕ' but only on the beam splitter parameter R , and N . For $R = 0.5$ it is symmetric in

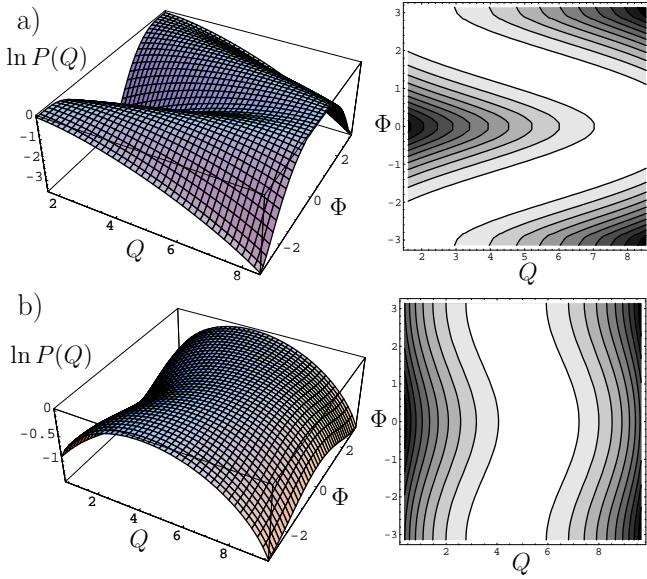


FIG. 6: The distribution function (logarithmic scale) at zero temperature under influence of decoherence ($N = 10$, $t_0 = 1$). (a) weak dephasing: $z = e^{0.32}$, (b) strong dephasing: $z = e^2$. The flux dependence is suppressed, and the distribution tends towards a symmetric function for $R = 0.5$.

and thus yields a symmetric contribution to the distribution function. The second part is the interference term proportional to $z \cos \phi$; for $R = 0.5$ it is asymmetric in Q .

In the general case for arbitrary z , we perform the Fourier transform of Eq. (15) numerically to find the distribution function $P(Q)$. Fig. 6 depicts the logarithm of the distribution function for weak (Fig. 6(a)) and strong dephasing (Fig. 6(b)) for a time interval $t_0 = 1$. In the case of weak dephasing, it still exhibits the form of a binomial distribution with the periodicity in Q (compare with the no-dephasing case in Fig. 2(a)). For increasing dephasing strength, the AB-effect is suppressed. In the case of symmetric beam splitters the function $P(Q)$ then tends towards a symmetric distribution around $N = 2$, and the third cumulant vanishes. However, for asymmetric beam splitters the distribution function is not symmetric.

To extract information about the tails of the distribution function $P(Q)$, we use the stationary phase approximation and solve the saddle point equation $\frac{d \ln h}{d i} = iQ$ for i in the complex plane. For $Q \gg i$, i.e. when nearly no particles are transferred to lead 3, we find $i \approx 1$ for negative Q . Starting from Eq. (16) we obtain

$$\ln P(Q) \approx Q \ln \left(\frac{v}{t_0} \right) + \frac{t_0}{2} \ln v - Q \ln \frac{v}{w} \quad (18)$$

The first term determines essentially the variation of the distribution function with Q . Only the parameter v and w are functions of the magnetic flux and the decoherence

parameter z :

$$v = \sum_{m=0}^N \sum_{p;q=0}^m V_{m,pq} X^m \quad (19)$$

$$w = \sum_{m=0}^N \sum_{p;q=0}^m V_{m,pq} \frac{N}{1} \frac{m+q}{q} \frac{2RT}{1} \frac{2RT}{2RT}$$

with

$$V_{m,pq} = \frac{N}{m} \frac{m}{p} \frac{N}{q} \frac{m}{q} \quad (20)$$

$$2^N (RT)^m q! (2RT)^{N-m+q} e^{-i(2p-m)} z^{(2p-m)^2} :$$

Thus in Eq. (18) the dominating contribution of the Q -dependence of $P(Q)$ is classical, and the last two terms represent the coherent part. For positive Q , the large Q tail, $Q \gg i$, of the distribution function is obtained in an analogous procedure.

VII. CONCLUSION

We analyze the Full Counting Statistics of a mesoscopic, electrical Mach-Zehnder interferometer penetrated by an Aharonov-Bohm flux, and in the presence of a classical fluctuating potential. The Mach-Zehnder interferometer has the advantage that there are no closed orbits. Interference is only a consequence of superposition of amplitudes in the out-going channels. Of interest is the generating function of transferred charge for such a quantum coherent conductor and the transition from coherent transport to classical transport.

First, we discuss the probability distribution for a fully coherent Mach-Zehnder interferometer. At zero temperature the distribution of transferred charge is binomial like in a two terminal conductor, but with a flux-dependent transmission probability. At finite temperature, the fact that we deal with a multi-terminal conductor leads to a different distribution which becomes classical due to flux-independent two-particle processes.

In the presence of a fluctuating potential, assuming that it is Gaussian, we obtain the first three cumulants as a function of the Aharonov-Bohm flux and a dephasing parameter. The classical fluctuating potential modulates the conductance. As a consequence the noise contains a term proportional to voltage squared. The same effect results in a term cubic in voltage in the third cumulant. In the third cumulant the conductance modulation is correlated as well with the shot noise. The cumulant of the k -th order shows oscillations in the flux up to $\cos k$. As one expects the high-order harmonics of the Aharonov-Bohm oscillations are suppressed much stronger with increasing dephasing than the low order oscillations.

For the limiting case of high voltage we find the generating function. This permits, like in the coherent case, the calculation of the distribution function of the transferred charge. Therefore, in this limiting case, we are able

to follow the suppression of the AB-oscillations in the distribution function.

For the tails of the distribution function we find that they consist of two parts: a purely classical part, independent of dephasing, which determines the dependence on transferred charge and a quantum part which governs the flux dependence.

The analysis of the conceptually simple case of a Mach-Zehnder interferometer will hopefully provide a useful point of reference for future theoretical investigations of Counting Statistics in the presence of quantum fluctuations. However, the Mach-Zehnder interferometer is not only of theoretical interest, but recently has been realized experimentally³². The questions addressed here are thus also of interest for future experiments.

Acknowledgments

We thank Eugene Sukhorukov for fruitful discussions. This work was supported by the Swiss National Science Foundation and the program for Materials with Novel Electronic Properties.

*

APPENDIX A: CALCULATION OF SINGLE CUMULANTS

Successive derivatives in $\ln g$ of the logarithm of the generating function, see Eq. (11), yield the cumulants. Using the expression (8) each cumulant is expressed in terms of derivatives of the matrix A , introduced in section IV. Derivatives of A of k -th order can be written in terms of a matrix $K = S^y P S$ and the matrix n , defined in section IV. P is a projection matrix with only non-vanishing element, $P_{33} = 1$. Note that K has non-vanishing elements only in the upper diagonal 2×2 block. Because backscattering is excluded in the MZI, the product $P K$ vanishes and we obtain the simple form

$$\frac{d^k A}{d^k z} = i^k n K + (-1)^k P : \quad (A1)$$

The matrix K is separated into constant matrices hK and L , and time-dependent scalar functions as follows: $K = hK + L(e^{i\varphi(t)} z) + L^y(e^{-i\varphi(t)} z)$. Here z is the decoherence parameter $z = e^{-i\varphi(t)}$, introduced in section V. The average is calculated by replacing the generating function in Eq. (9) by the phase factor; at this point we explicitly assume a Gaussian fluctuating potential $U(t)$, and use R_C .

The average of the matrix K is denoted by $\langle hK \rangle$, it is determined only by the parameters R , γ , and z . The averaging of the cumulants only affects the time-dependent functions $(e^{i\varphi(t)} z)$: Depending on the order k of the cumulants one obtains products of the functions $(e^{i\varphi(t)} z)$ at k different times. The averaging then defines correlation functions of different order.

In the noise we get two correlation functions, depending on one time variable and determined by the parameter z :

$$g(t) = \frac{1}{z^2} \langle e^{i\varphi(t)} z \rangle \langle e^{i\varphi(0)} z \rangle = \langle z^{-2(1-\frac{\gamma}{2})} \rangle : \quad (A2)$$

The procedure of the average is similar to the calculation of the parameter z .

For the third cumulant four correlations functions h_+ depending on two time variables are possible, for example

$$h_+(t; t^0) = \frac{1}{z^3} \langle e^{i\varphi(t)} z \rangle \langle e^{i\varphi(t^0)} z \rangle \langle e^{i\varphi(0)} z \rangle : \quad (A3)$$

The functions $h(t; t^0)$ can be expressed in terms of g given by Eq. (A2).

With Eqs. (11) and (A1) all cumulants take a compact form. The mean current in lead 3 is

$$hI_3 = \frac{1}{it_0} \text{Tr} \frac{dA}{d} = \frac{1}{t_0} \text{Tr} [n hK] : \quad (A4)$$

leading to the result presented in section V.

For the noise we express the second cumulant in terms of derivatives of A , taken at $t = 0$:

$$C^2 = \frac{1}{i^2 t_0^2} \text{Tr} \frac{dA}{d} \text{Tr} \frac{dA}{d} + \frac{1}{i^2 t_0^2} \text{Tr} \frac{d^2 A}{d^2} : \quad (A5)$$

The first term corresponds to the modulation noise I_1 and disappears in the case of no dephasing. The second term is the two-particle contribution (that separates into n_{nyq} and n_{ex} as explained in section V). Introducing the K -matrix, Eq. (A5) simplifies to

$$C^2 = \frac{1}{t_0^2} (\text{Tr} [n hK] n hK)^2 + \frac{1}{t_0^2} \text{Tr} [n hK (1 - n) K] : \quad (A6)$$

since the product $K(1 - K)$ vanishes. The final result contains the Fourier transforms of the functions g and a frequency integral, as also found in Ref. [33].

As for the current and the noise, we express the third cumulant in terms of derivatives of A at $t = 0$:

$$C^3 = \frac{1}{i^3 t_0^3} \text{Tr} \frac{dA}{d} \text{Tr} \frac{dA}{d} \text{Tr} \frac{dA}{d} + 3 \text{Tr} \frac{dA}{d} \text{Tr} \frac{dA}{d} \text{Tr} \frac{d^2 A}{d^2} + \text{Tr} \frac{d^3 A}{d^3} + 2 \text{Tr} \frac{dA}{d} \text{Tr} \frac{d^2 A}{d^2} : \quad (A7)$$

The first term corresponds to the modulation contribution C_I^3 , the second term to the term C_I^3 , and the remaining part gives the three-particle contribution C_{3p}^3 . One checks immediately, that the first two terms vanish in the absence of dephasing. Using again the compact expressions in K, Eq. (A 7) becomes

$$C^3 = \frac{1}{t_0} \frac{hD}{D} (\text{Tr}[\hat{n}K - n\hat{h}K])^3 + \frac{E}{E_I} + 3 \frac{E}{D} (\text{Tr}[\hat{n}K - n\hat{h}K]) (\text{Tr}[\hat{n}K (1 - n)K]) + \text{Tr}[\hat{n}K (1 - n)K (1 - 2n)K] : \quad (\text{A } 8)$$

The evaluation of Eq. (A 8) is quite lengthy. Introducing Fourier transforms of the correlation functions h and g and of the occupation functions n describing the leads, one is left with an integral over two frequencies. This integral contains a convolution of h or g with temperature and voltage dependent kernels. We evaluate the integration numerically.

The limiting cases were introduced in section V. In the high voltage regime, the accumulated phase varies slowly. Therefore, we evaluate the correlation functions g and h (see Eqs. (A 2) and (A 3)) at equal times:

$$\text{slow : } \begin{matrix} g(t) & g(0) \\ h(t; t^0) & h(0; 0): \end{matrix} \quad (\text{A } 9)$$

In this limit the correlation functions are entirely determined by the parameter z . The frequency integrals in the final expression of C_{3p}^3 are given by integrands at zero frequency and thus simplify substantially. As the modulation term C_I^3 does not depend on the phase dynamics, it does not change in this approximation. The term C_I^3 combines a modulation part and a two-particle process. Here we use $h(t; t^0) \rightarrow h(0; t^0)$.

The high voltage approximation does not catch contributions to the third cumulant due to particle-hole excitations created by the fluctuating potential $U(t)$. Similar to Ref. [33], this leads to an unimportant linear offset between the exact result and the high voltage result. For better comparison, this offset is subtracted in Fig. 5, which shows a good agreement of the high voltage approximation with the exact result.

In the opposite case, for low voltage, the phase factors in formula (A 2) and (A 3) at different times are uncorrelated and thus can be averaged independently and vanish. In this case, we use in C_{3p}^3 the approximation

$$\text{fast : } \begin{matrix} g(t) & 0 \\ h(t; t^0) & 0: \end{matrix} \quad (\text{A } 10)$$

C_I^3 is proportional to V^3 and thus in the low voltage regime small compared to the terms linear in voltage. For low temperature also the contribution C_I^3 is negligible.

-
- ¹ Y. M. Blanter and M. Buttiker, *Physics Reports* 336 (2000).
 - ² V. A. Khlus, *Zh. Eksp. Teor. Fiz.* 93, 2179 (1987).
 - ³ G. B. Lesovik, *Pis'ma Zh. Eksp. Teor. Fiz.* 49, 513 (1989).
 - ⁴ M. Buttiker, *Phys. Rev. Lett.* 65, 2901 (1990).
 - ⁵ M. Buttiker, *Phys. Rev. B* 46, 12485 (1992).
 - ⁶ L. S. Levitov, H. Lee, and G. B. M. Lesovik, *J. Math. Phys.* 37, 4845 (1996).
 - ⁷ L. S. Levitov and G. B. Lesovik, *Pis'ma Zh. Eksp. Teor. Fiz.* 58 (1993).
 - ⁸ Y. V. Nazarov, *Ann. Phys. (Leipzig)* 8 (1999).
 - ⁹ W. Belzig and Y. V. Nazarov, *Phys. Rev. Lett.* 87, 197006 (2001).
 - ¹⁰ W. Belzig and Y. V. Nazarov, *Phys. Rev. Lett.* 87, 067006 (2001).
 - ¹¹ Y. V. Nazarov and D. A. Bagrets, *Phys. Rev. Lett.* 88, 196801 (2002).
 - ¹² D. B. Gutman, A. D. Mirlin, and Y. Gefen, *cond-mat/0403436* (2004).
 - ¹³ K. E. Nagaev, *Phys. Rev. B* 66, 075334 (2002).
 - ¹⁴ S. Pilgram, A. N. Jordan, E. V. Sukhorukov, and M. Buttiker, *Phys. Rev. Lett.* 90, 206801 (2003).
 - ¹⁵ S. Pilgram, *Phys. Rev. B* 69, 115315 (2004).
 - ¹⁶ K. E. Nagaev, S. Pilgram, and M. Buttiker, *Phys. Rev. Lett.* 92, 176804 (2004).
 - ¹⁷ S. Pilgram, K. E. Nagaev, and M. Buttiker, *Phys. Rev. B* 70, 045304 (2004).
 - ¹⁸ A. N. Jordan, E. V. Sukhorukov, and S. Pilgram, *J. Math. Phys.* 45, 4386 (2004).
 - ¹⁹ A. N. Jordan and E. V. Sukhorukov, *Phys. Rev. Lett.* 93, 260604 (2004).
 - ²⁰ E. V. Sukhorukov and O. M. Bulashenko, *cond-mat/0408075* (2004).
 - ²¹ T. Bodineau and B. Derrida, *Phys. Rev. Lett.* 92, 180601 (2004).
 - ²² L. Bertini, A. De Sole, D. Gabrielli, G. Jona-Lasino, and C. Landim, *Phys. Rev. Lett.* 94, 030601 (2005).
 - ²³ B. Reulet, J. Senzier, and D. E. Prober, *Phys. Rev. Lett.* 91, 196601 (2003).
 - ²⁴ M. Kindermann, Y. V. Nazarov, and C. W. J. Beenakker, *Phys. Rev. B* 69, 035336 (2003).
 - ²⁵ J. Tobiska and Y. V. Nazarov, *Phys. Rev. Lett.* 93, 106801 (2004).
 - ²⁶ T. T. Heikkilä, P. Virtanen, G. Johansson, and F. K. Wilhelm, *Phys. Rev. Lett.* 93, 247005 (2004).
 - ²⁷ J. Pekola, *Phys. Rev. Lett.* 93, 206601 (2004).
 - ²⁸ G. Seelig and M. Buttiker, *Phys. Rev. B* 64 (2001).
 - ²⁹ G. Seelig, S. Pilgram, A. N. Jordan, and M. Buttiker, *Phys. Rev. B* 68 (2003).
 - ³⁰ A. E. Hansen, A. Kristensen, S. Pedersen, C. P. Sørensen, and P. E. Lindelof, *Phys. Rev. B* 64 (2001).
 - ³¹ K. Kobayashi, H. Aikawa, S. Katsumoto, and Y. Iye, *J. Phys. Soc. Jpn.* 71, 2094 (2002).
 - ³² Y. Ji, Y. Chung, D. Sprinzak, M. Heiblum, D. Mahalu, and H. Shtrikman, *Nature* 422, 415 (2003).
 - ³³ F. Marquardt and C. Bruder, *Phys. Rev. Lett.* 92 (2004); *Phys. Rev. B* 70, (2004).
 - ³⁴ F. Marquardt, *cond-mat/0410333* (2004).

